
KEK preprint 2001-2
Belle preprint 2001-3



# Measurement of Inclusive Production of Neutral Pions from $\Upsilon(4S)$ Decays

**Belle Collaboration**

K. Abe,[1] K. Abe,[2] I. Adachi,[1] Byoung Sup Ahn,[3] H. Aihara,[4] M. Akatsu,[5] G. Alimonti,[6] K. Aoki,[1] K. Asai,[7] Y. Asano,[8] T. Aso,[9] V. Aulchenko,[10] T. Aushev,[11] A. M. Bakich,[12] E. Banas,[13] W. Bartel,[1,14] S. Behari,[1] P. K. Behera,[15] D. Beiline,[10] A. Bondar,[10] A. Bozek,[13] T. E. Browder,[6] B. C. K. Casey,[6] P. Chang,[16] Y. Chao,[16] B. G. Cheon,[17] S.-K. Choi,[18] Y. Choi,[17] Y. Doi,[1] J. Dragic,[19] A. Drutskoy,[11] S. Eidelman,[10] Y. Enari,[5] R. Enomoto,[1,20] F. Fang,[6] H. Fujii,[1] C. Fukunaga,[21] M. Fukushima,[20] A. Garmash,[10,1] A. Gordon,[19] K. Gotow,[22] H. Guler,[6] R. Guo,[23] J. Haba,[1] H. Hamasaki,[1] K. Hanagaki,[24] F. Handa,[2] K. Hara,[25] T. Hara,[25] T. Haruyama,[1] N. C. Hastings,[19] K. Hayashi,[1] H. Hayashii,[7] M. Hazumi,[25] E. M. Heenan,[19] Y. Higasino,[5] I. Higuchi,[2] T. Higuchi,[4] H. Hirano,[26] T. Hojo,[25] Y. Hoshi,[27] W.-S. Hou,[16] S.-C. Hsu,[16] H.-C. Huang,[16] Y.-C. Huang,[23] S. Ichizawa,[28] Y. Igarashi,[1] T. Iijima,[1] H. Ikeda,[1] K. Ikeda,[7] K. Inami,[5] A. Ishikawa,[5] H. Ishino,[28] R. Itoh,[1] G. Iwai,[29] H. Iwasaki,[1] Y. Iwasaki,[1] D. J. Jackson,[25] P. Jalocha,[13] H. K. Jang,[30] M. Jones,[6] R. Kagan,[11] H. Kakuno,[28] J. Kaneko,[28] J. H. Kang,[31] J. S. Kang,[3] P. Kapusta,[13] N. Katayama,[1] H. Kawai,[32] N. Kawamura,[33] T. Kawasaki,[29] H. Kichimi,[1] D. W. Kim,[17] Heejong Kim,[31] H. J. Kim,[31] Hyunwoo Kim,[3] S. K. Kim,[30] K. Kinoshita,[34] K. Korotushenko,[24] P. Krokovny,[10] R. Kulasiri,[34] S. Kumar,[35] T. Kuniya,[36] E. Kurihara,[32] A. Kuzmin,[10] Y.-J. Kwon,[31] J. S. Lange,[37] M. H. Lee,[1] S. H. Lee,[30] H.B. Li,[38] D. Liventsev,[11] R.-S. Lu,[16] A. Manabe,[1] T. Matsubara,[4] S. Matsui,[5] S. Matsumoto,[39] T. Matsumoto,[5] Y. Mikami,[2] K. Misono,[5] K. Miyabayashi,[7] H. Miyake,[25] H. Miyata,[29] L. C. Moffitt,[19] G. R. Moloney,[19] G. F. Moorhead,[19] S. Mori,[8] A. Murakami,[36] T. Nagamine,[2] Y. Nagasaka,[40] Y. Nagashima,[25] T. Nakadaira,[4] E. Nakano,[41] M. Nakao,[1] J. W. Nam,[17] S. Narita,[2] Z. Natkaniec,[13] K. Neichi,[27] S. Nishida,[42] O. Nitoh,[26] S. Noguchi,[7] T. Nozaki,[1] S. Ogawa,[43] T. Ohshima,[5] Y. Ohshima,[28] T. Okabe,[5] T. Okazaki,[7] S. Okuno,[44] S. L. Olsen,[6] W. Ostrowicz,[13] H. Ozaki,[1] H. Palka,[13] C. S. Park,[30] C. W. Park,[3] H. Park,[3] L. S. Peak,[12] M. Peters,[6] L. E. Piilonen,[22] E. Prebys,[24] J. L. Rodriguez,[6] N. Root,[10] M. Rozanska,[13] K. Rybicki,[13] J. Ryuko,[25] H. Sagawa,[1] Y. Sakai,[1] H. Sakamoto,[42] M. Satapathy,[15] A. Satpathy,[1,34] S. Schrenk,[22,34] S. Semenov,[11] K. Senyo,[5] M. E. Sevior,[19] H. Shibuya,[43] B. Shwartz,[10] V. Sidorov,[10] J.B. Singh,[35] S. Stanič,[8] A. Sugi,[5] A. Sugiyama,[5] K. Sumisawa,[25] T. Sumiyoshi,[1] K. Suzuki,[32] S. Suzuki,[5] S. Y. Suzuki,[1] S. K. Swain,[6]

T. Takahashi,[41] F. Takasaki,[1] M. Takita,[25] K. Tamai,[1] N. Tamura,[29] J. Tanaka,[4] M. Tanaka,[1] Y. Tanaka,[40] G. N. Taylor,[19] Y. Teramoto,[41] M. Tomoto,[5] T. Tomura,[4] S. N. Tovey,[19] K. Trabelsi,[6] T. Tsuboyama,[1] Y. Tsujita,[8] T. Tsukamoto,[1] S. Uehara,[1] K. Ueno,[16] Y. Unno,[32] S. Uno,[1] Y. Ushiroda,[42] Y. Usov,[10] S. E. Vahsen,[24] G. Varner,[6] K. E. Varvell,[12] C. C. Wang,[16] C. H. Wang,[45] M.-Z. Wang,[16] T.J. Wang,[38] Y. Watanabe,[28] E. Won,[30] B. D. Yabsley,[1] Y. Yamada,[1] M. Yamaga,[2] A. Yamaguchi,[2] H. Yamamoto,[6] H. Yamaoka,[1] Y. Yamaoka,[1] Y. Yamashita,[46] M. Yamauchi,[1] S. Yanaka,[28] K. Yoshida,[5] Y. Yusa,[2] H. Yuta,[33] C.C. Zhang,[38] J. Zhang,[8] Y. Zheng,[6] V. Zhilich,[10] and D. Žontar[8]

[1]*High Energy Accelerator Research Organization (KEK), Tsukuba*

[2]*Tohoku University, Sendai*

[3]*Korea University, Seoul*

[4]*University of Tokyo, Tokyo*

[5]*Nagoya University, Nagoya*

[6]*University of Hawaii, Honolulu HI*

[7]*Nara Women's University, Nara*

[8]*University of Tsukuba, Tsukuba*

[9]*Toyama National College of Maritime Technology, Toyama*

[10]*Budker Institute of Nuclear Physics, Novosibirsk*

[11]*Institute for Theoretical and Experimental Physics, Moscow*

[12]*University of Sydney, Sydney NSW*

[13]*H. Niewodniczanski Institute of Nuclear Physics, Krakow*

[14]*Deutsches Elektronen–Synchrotron, Hamburg*

[15]*Utkal University, Bhubaneswer*

[16]*National Taiwan University, Taipei*

[17]*Sungkyunkwan University, Suwon*

[18]*Gyeongsang National University, Chinju*

[19]*University of Melbourne, Victoria*

[20]*Institute for Cosmic Ray Research, University of Tokyo, Tokyo*

[21]*Tokyo Metropolitan University, Tokyo*

[22]*Virginia Polytechnic Institute and State University, Blacksburg VA*

[23]*National Kaohsiung Normal University, Kaohsiung*

[24]*Princeton University, Princeton NJ*

[25]*Osaka University, Osaka*

[26]*Tokyo University of Agriculture and Technology, Tokyo*

[27]*Tohoku Gakuin University, Tagajo*

[28]*Tokyo Institute of Technology, Tokyo*

[29]*Niigata University, Niigata*

[30]*Seoul National University, Seoul*

[31]*Yonsei University, Seoul*

[32]*Chiba University, Chiba*

[33]*Aomori University, Aomori*

[34]*University of Cincinnati, Cincinnati, OH*

[35]*Panjab University, Chandigarh*

[36]*Saga University, Saga*

[37] *University of Frankfurt, Frankfurt*
[38] *Institute of High Energy Physics, Chinese Academy of Sciences, Beijing*
[39] *Chuo University, Tokyo*
[40] *Nagasaki Institute of Applied Science, Nagasaki*
[41] *Osaka City University, Osaka*
[42] *Kyoto University, Kyoto*
[43] *Toho University, Funabashi*
[44] *Kanagawa University, Yokohama*
[45] *National Lien-Ho Institute of Technology, Miao Li*
[46] *Nihon Dental College, Niigata*
(Dated: March 24, 2001)

## Abstract

Using the Belle detector operating at the KEKB $e^+e^-$ storage ring, we have measured the mean multiplicity and the momentum spectrum of neutral pions from the decays of the $\Upsilon(4S)$ resonance. We measure a mean of $4.70 \pm 0.04 \pm 0.22$ neutral pions per $\Upsilon(4S)$ decay.

This analysis presents the first results on the average multiplicity of neutral pions and their momentum spectrum in $B$ meson decays at the $\Upsilon(4S)$ resonance using the Belle detector [1] at KEKB [2]. The measurement is based on the sample of $3.4 \times 10^6$ $B$ meson pairs collected by the Belle detector at a center-of-mass (CM) energy of $\sqrt{s} = 10.58\,\mathrm{GeV}$.

The particle composition of hadronic final states in $e^+e^-$ annihilation and the measurement of inclusive particle production rates have been important subjects for various energy regions. Previous studies of particle composition at the $\Upsilon(4S)$ resonance include measurements of charged particles ($\pi^\pm$ [3, 4] and $K^\pm$ [5, 6]), $\eta$ mesons [7], and vector mesons [8, 9]. For typical $B$ meson decays, the bulk of the neutral energy is carried by neutral pions. Measurements of inclusive spectra contain information on $B$ meson decay mechanisms, especially in the high momentum region where important rare decays may become detectable. If the details of these inclusive spectra are known more precisely, they will allow better estimation of backgrounds and better modeling of $B$ meson decay.

The Belle detector (see Fig. 1), described in detail in Ref. [1], consists of a silicon vertex detector (SVD) [10], central drift chamber (CDC) [11], aerogel Čerenkov counter (ACC) [12], time of flight/trigger scintillation counter (TOF/TSC) [13], CsI electromagnetic calorimeter (ECL) [14] and $\mathrm{K}_L$/muon detector (KLM) [15]. The SVD measures the precise position of decay vertices. It consists of three layers of double-sided silicon strip detectors (DSSD) in a barrel-only design and covers 86% of the solid angle. The layer radii are 3.0, 4.5, and 6.0 cm. Charged tracks are reconstructed primarily by the CDC that covers the $17^\circ < \theta < 150^\circ$ polar angular region. It consists of 50 cylindrical layers of drift cells organized into 11 super-layers (axial or small-angle-stereo), each containing between three and six layers. A low $Z$ gas mixture (50% He, 50% $\mathrm{C_2H_6}$) is used to minimize multiple-Coulomb scattering. The inner and outer radii of the CDC are 9 cm and 86 cm, respectively. The solenoidal magnetic field of 1.5 Tesla is chosen to optimize momentum resolution without sacrificing reconstruction efficiency for low momentum tracks. Kaon identification (KID) is provided by specific ionization ($dE/dx$) measurements in the CDC, Čerenkov threshold measurements in the ACC, and the cylindrical TOF scintillator barrel. The ECL is made of finely segmented CsI(T$\ell$) crystals 30 cm in length. The cross section of one counter is approximately $55 \times 55$ mm$^2$ at the front surface. The ECL crystals cover the $12^\circ < \theta < 157^\circ$ angular region. The inner radius of the barrel is 1.25 m, while the annular endcaps are placed at +2.0 m and $-1.0$ m along the beam line from the interaction point. The calibration of the calorimeter is performed using cosmic rays and Bhabha events. The KLM consists of alternating layers of glass resistive plate counters and 4.7 cm thick iron plates.

The data samples used in this analysis correspond to $3.2\,\mathrm{fb}^{-1}$ of integrated luminosity taken at the $\Upsilon(4S)$ resonance and $0.6\,\mathrm{fb}^{-1}$ taken at a CM energy 60 MeV below the resonance; the latter was used to subtract underlying continuum background. The integrated luminosity was determined from the number of Bhabha events for which we require both electron and positron in the region of $46.7^\circ < \theta^* < 145.7^\circ$ in the center-of-mass frame.

Hadronic events are selected based on charged track information from the CDC and cluster information from the ECL. We require at least three charged tracks, that the energy sum in the calorimeter be between 10% and 80% of $\sqrt{s}$, and that the charged track momentum be balanced in the $z$ direction. This removes the majority of two photon, radiative Bhabha, and $\tau^+\tau^-$ events where both $\tau$'s decay to leptons. Radiative Bhabha events with one electron outside of the ECL acceptance are removed by requiring at least one large-angle cluster in the ECL and requiring that the average cluster energy be below 1 GeV. Higher multiplicity $\tau^+\tau^-$ events are removed if the charged and neutral energy sums in the event are

consistent with a $\tau$ pair event and if the reconstructed invariant mass of the particles found in each of the two hemispheres perpendicular to the event thrust axis falls below the $\tau$ mass. Beam-gas and beam-wall backgrounds are removed by reconstructing the primary vertex of the event and requiring it to be consistent with the known location of the interaction point. The selection is 99% efficient for $B\bar{B}$ events and approximately 87% efficient for continuum events. The efficiency for the hadronic event selection was found by a GEANT-based [16] Monte Carlo simulation program. To suppress continuum, we require that the ratio $R_2$ of second to zeroth Fox-Wolfram moments [17], determined using charged tracks and neutral clusters, be less than 0.5.

Photons are reconstructed from neutral clusters in the ECL that have a lateral shape consistent with that of an electromagnetic shower. The energy resolution was measured to be $\sigma_E/E = 0.066\%/E \oplus 0.81\%/E^{0.25} \oplus 1.34\%$ ($E$ in GeV) from beam tests [14]. To keep the combinatorial background at a reasonable level, only photons in the central barrel region ($35^\circ < \theta < 120^\circ$) with $E_\gamma \geq 30\,\mathrm{MeV}$ are used in this analysis; the endcap regions have worse energy resolution due to more intervening material and higher beam-associated background.

For each 100 MeV/$c$ momentum bin in the CM momentum range 0 to 3 GeV/$c$, the $\gamma\gamma$ invariant mass distribution is fit to an asymmetric (symmetric above 2 GeV/$c$) Gaussian (i.e., a Gaussian with different widths on either side of the mean) for the signal plus a polynomial for the combinatorial background to extract the $\pi^0$ yields. Fig. 2 shows typical mass spectra obtained from the on-resonance data. For the asymmetric Gaussians, the mass resolution is defined as the mean of the left- and right-hand sigmas. An average mass resolution of 5 MeV/$c^2$ is obtained, dominated by energy resolution at low momenta or by angular resolution at high momenta. The mass peak is shifted slightly from the established value [18] because of the asymmetric energy response of the calorimeter due to shower leakage. The observed mass peak position and resolution are consistent with Monte Carlo expectations, as shown in Fig. 3.

To extract the $\pi^0$ momentum spectrum from $\Upsilon(4S)$ decays, the underlying continuum in the on-resonance data is subtracted bin-by-bin using off-resonance data. The inclusive spectrum is calculated using

$$\frac{1}{\sigma_h} \cdot \frac{d\sigma_{\pi^0}}{dp^*_{\pi^0}} = \frac{1}{N_h} \cdot \frac{Y^i_{\mathrm{on}} - \alpha \cdot Y^i_{\mathrm{off}}}{\epsilon^i \cdot \Delta p^*_{\pi^0}} \ , \tag{1}$$

where $N_h$ is the number of produced $B\bar{B}$ events, $Y_{\mathrm{on}}$ and $Y_{\mathrm{off}}$ are the background-subtracted $\pi^0$ yields obtained from on- and off-resonance data fits, $\alpha = (\mathcal{L}_{\mathrm{on}}/\mathcal{L}_{\mathrm{off}}) \cdot (s_{\mathrm{off}}/s_{\mathrm{on}})$ is the on-off scaling factor, and $\epsilon$ is the product of acceptance and detection efficiency for each momentum bin. The average $\pi^0$ multiplicity is obtained by summing the data from the measured individual momentum bins as shown in Table I.

The $\pi^0$ acceptance and detection efficiency are determined from Monte Carlo simulations of $B\bar{B}$ decays (equal proportions of charged and neutral $B$ mesons) and continuum processes. The $\gamma\gamma$ invariant mass distributions are fit with the same functions as used in the real data analysis. The product of acceptance and detection efficiency are defined as the ratio of the fitted $\pi^0$ yield to the generated count. Efficiencies for the high momentum $\pi^0$'s above the kinematic limit for $B\bar{B}$ decays are deduced from continuum Monte Carlo normalized in the 2.2–2.3 GeV/$c$ bin, and scaled efficiencies are used that account for the different acceptances.

Possible sources of systematic uncertainties and their effect on the inclusive $\pi^0$ mean multiplicity measurement are summarized in Table II. These are discussed next.

The uncertainties in the number of $B\bar{B}$ events and the hadronic event selection efficiency are estimated to be 1% and 1.1%, respectively, or 1.5% combined.

The effect of uncertainty in the relative luminosity ratio, used to subtract the continuum background from the on-resonance data, was studied by varying the size of the continuum subtraction by 1%, and we find a 1.5% uncertainty in the mean multiplicity.

Due to the CM energy difference between on- and off-resonance data, the characteristics of continuum events may not match, leading to a bias in the continuum subtraction from the on-resonance data. In particular, the event shape at lower CM energy is slightly less jet-like so that more continuum events survive the common $R_2$ cut (resulting in an oversubtraction from the on-resonance data), and the particle momenta scale with CM energy. Hadronic event selection and $R_2$ cut bias from the on-off energy difference were determined by using a continuum Monte Carlo [19] sample generated at the CM energy of the off-resonance data; we estimate a 0.4% uncertainty in the $\pi^0$ multiplicity due to this effect. Particle momentum scaling with CM energy was studied by comparing the multiplicity with and without momentum scaling; this leads to an uncertainty of 0.3%.

The uncertainties in the $\pi^0$ detection efficiency due to the application of the shower transverse shape cut, the charged-track veto, photon energy smearing, and the ECL's modest non-linear energy response correction, are estimated to be 0.4%, 1.6%, 2%, and 0.6%, respectively (determined by comparing the yields with and without each of these criteria).

The decay angular distribution for the photons in the $\pi^0$ rest frame is expected to be isotropic, but the detected distribution of the decay angle $\theta_d$— defined as the angle between the photon momentum in the $\pi^0$ rest frame and the $\pi^0$ momentum in the laboratory frame— shows an energy dependence due to the $\gamma$ energy cut. Inaccuracy in the Monte Carlo simulation could manifest itself as an anisotropy in the efficiency-corrected decay angle distribution. A comparison between Monte Carlo and data for $|\cos\theta_d| > 0.5$ and $|\cos\theta_d| \leq 0.5$ shows no discrepancy and is used to estimate a systematic uncertainty of 0.3%.

The $\gamma\gamma$ invariant mass distribution for each CM momentum bin is fit to the following functions in the mass window 80–180 MeV/$c^2$:

- $p^*_{\gamma\gamma} < 1.0$ GeV/$c$: 4th order polynomial plus asymmetric Gaussian;
- $1.0 \leq p^*_{\gamma\gamma} < 2.0$ GeV/$c$: 2nd order polynomial plus asymmetric Gaussian;
- $2.0 \leq p^*_{\gamma\gamma} < 3.0$ GeV/$c$: 2nd order polynomial plus Gaussian.

The fitting range and the order of the polynomial are chosen to minimize statistical fluctuation. By changing the order of the polynomial, the relative yield variation between data and Monte Carlo is taken as the systematic uncertainty in the background modeling; a 2.8% uncertainty was deduced. The weighted average of the fit errors in the efficiency estimation, $(\delta\epsilon)^2 = \sum_i \sigma^2_{\epsilon,i} \cdot Y_i^{\pi^0} / \sum_i Y_i^{\pi^0}$, leads to 1% uncertainty in the $\pi^0$ multiplicity. Combining these two numbers gives a 3% systematic uncertainty in the $\pi^0$ mean multiplicity measurement due to the fit procedure.

The measured $\pi^0$ momentum spectrum is compared to the $B\bar{B}$ Monte Carlo [20] prediction in Fig. 4. Systematic differences in the intermediate momentum region may be caused by overestimation of $b \to c$ processes in the Monte Carlo event generation: 100% $b \to c$ is assumed for generic $B\bar{B}$ decays in our Monte Carlo. In the high momentum region above the $b \to c$ kinematic end point, we searched for a $\pi^0$ excess from charmless $B$ decays. We find $N_{\rm excess} = 410 \pm 724$ events in the momentum interval 2.4–2.7 GeV/$c$, which corresponds to a partial branching fraction $\mathcal{B}(B \to \pi^0 X;\ p > 2.4\,{\rm GeV}/c) = (2 \pm 3.5 \pm 6.7) \times 10^{-4}$, or less

than $1.4 \times 10^{-3}$ at 90% confidence level. However, the statistical precision here is limited and the fluctuations are dominated by the off-resonance data used in the subtraction.

In conclusion, using 3.2 fb$^{-1}$ of data accumulated at the $\Upsilon(4S)$ resonance by the Belle detector, we have measured the inclusive spectrum of neutral pions from $\Upsilon(4S)$ decays. By summing the measured momentum bins, the mean multiplicity of neutral pions from $\Upsilon(4S)$ decays has been determined to be $\langle n_{\pi^0} \rangle = 4.70 \pm 0.04 \pm 0.22$, corresponding to an inclusive branching fraction[21] of $\mathcal{B}(B \to \pi^0 X) = (235 \pm 2 \pm 11)\%$, where the first error is statistical and the second is systematic.

## ACKNOWLEDGMENTS

We gratefully acknowledge the efforts of the KEKB group in providing us with excellent luminosity and running conditions and the members of the KEK computing research center for their assistance with our computing and network systems. We thank the staffs of KEK and collaborating institutions for their contributions to this work, and acknowledge support from the Ministry of Education, Science, Sports and Culture of Japan and the Japan Society for the Promotion of Science; the Australian Research Council and the Australian Department of Industry, Science and Resources; the Department of Science and Technology of India; the BK21 program of the Ministry of Education of Korea and the Basic Science program of the Korea Science and Engineering Foundation; the Polish State Committee for Scientific Research under contract No.2P03B 17017; the Ministry of Science and Technology of Russian Federation; the National Science Council and the Ministry of Education of Taiwan; the Japan-Taiwan Cooperative Program of the Interchange Association; and the U.S. Department of Energy.

## REFERENCES

[1] Belle Technical Design Report, KEK Report 95-1, April 1995.
[2] KEKB B-Factory Design Report, KEK Report 95-7, August 1995.
[3] CLEO Collaboration, M. S. Alam *et al.*, Phys. Rev. Lett. **49**, 357 (1982).
[4] ARGUS Collaboration, H. Albrecht *et al.*, Z. Phys. **C58**, 191 (1993).
[5] CLEO Collaboration, M. S. Alam *et al.*, Phys. Rev. Lett. **58**, 1814 (1987).
[6] ARGUS Collaboration, H. Albrecht *et al.*, Z. Phys. **C62**, 371 (1994).
[7] CLEO Collaboration, Y. Kubota *et al.*, Phys. Rev. **D53**, 6033 (1996).
[8] CLEO Collaboration, D. Bortoletto *et al.*, Phys. Rev. Lett. **56**, 800 (1986).
[9] ARGUS Collaboration, H. Albrecht *et al.*, Z. Phys. **C61**, 1 (1994).
[10] G. Alimonti *et al.*, Nucl. Instrum. Methods Phys. Res., Sect. A **453**, 71 (2000).
[11] H. Hirano *et al.*, Nucl. Instrum. Methods Phys. Res., Sect. A **455**, 294 (2000); M. Akatsu *et al.*, Nucl. Instrum. Methods Phys. Res., Sect. A **454**, 322 (2000).
[12] T. Iijima *et al.*, Nucl. Instrum. Methods Phys. Res., Sect. A **453**, 321 (2000).
[13] H. Kichimi *et al.*, Nucl. Instrum. Methods Phys. Res., Sect. A **453**, 315 (2000).
[14] H. Ikeda *et al.*, Nucl. Instrum. Methods Phys. Res., Sect. A **441**, 401 (2000).
[15] A. Abashian *et al.*, Nucl. Instrum. Methods Phys. Res., Sect. A **449**, 112 (2000).
[16] R. Brun, F. Bruyant, M. Maire, A. C. McPherson and P. Zanarini, CERN-DD/EE/84-1.
[17] G. Fox and S. Wolfram, Phys. Rev. Lett. **41**, 1581 (1978).
[18] D. E. Groom *et al.*, Eur. Phys. J. **C15**, 1 (2000).

[19] T. Sjöstrand, "PYTHIA 5.6 and JETSET 7.3: Physics and manual," CERN-TH-6488-92.
[20] 'QQ – The CLEO Event Generator,' http://www.lns.cornell.edu/public/CLEO/soft/QQ (unpublished).
[21] Inclusive branching fractions in $B$ decays have a definition in terms of multiplicity and can be greater than 100% [18].

**FIGURES**

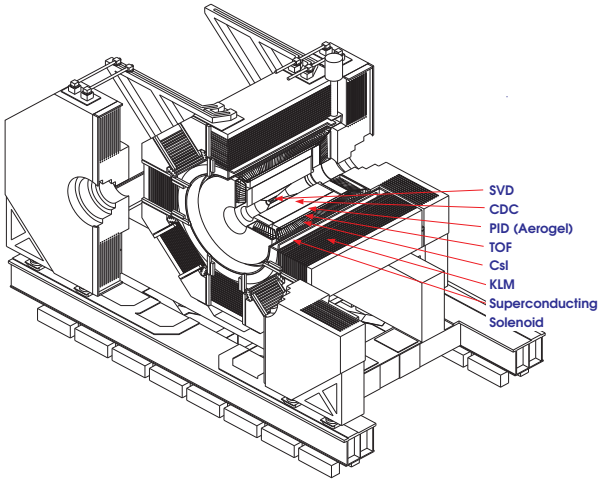


FIG. 1: Isometric cutaway view of the Belle detector.

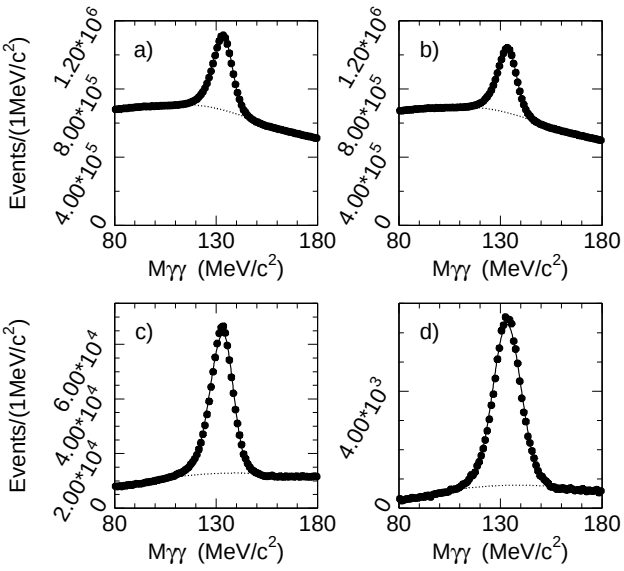


FIG. 2: $\gamma\gamma$ invariant mass distributions for the $\Upsilon(4S)$ resonance data. (a) $p^*_{\gamma\gamma} = 0.0$–$3.0$ GeV/$c$; (b) 0.0–1.0 GeV/$c$; (c) 1.0–2.0 GeV/$c$; (d) 2.0–3.0 GeV/$c$. An average mass resolution of 5 MeV/$c^2$ was obtained. The smooth curve in each plot is a fit to the data using an asymmetric (or symmetric) Gaussian plus a polynomial.

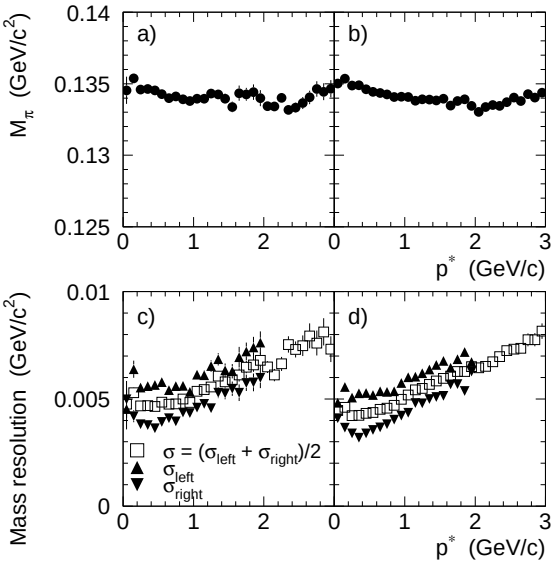


FIG. 3: Mass peak position and resolution obtained from off-resonance data and Monte Carlo expectations. (a),(c) data; (b),(d) continuum Monte Carlo. The fluctuations near 2 GeV/$c$ are caused by the change in the signal fitting function from an asymmetric to a symmetric Gaussian.

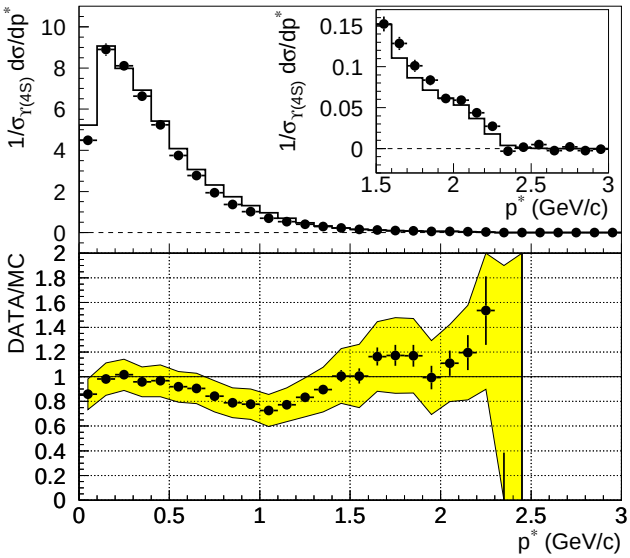


FIG. 4: Measured inclusive $\pi^0$ momentum spectrum in $\Upsilon(4S)$ decays, with the high momentum range shown in the inset. The histograms show the Monte Carlo prediction. The error bars are statistical, while the shaded band indicates one standard deviation systematic uncertainties.

**TABLES**

TABLE I: Measured inclusive $\pi^0$ spectrum from $\Upsilon(4S)$ decays, using $3.2\,\mathrm{fb}^{-1}$ on-resonance and $0.6\,\mathrm{fb}^{-1}$ off-resonance data.

| $p^*$ (GeV/$c$) | $Y_{\mathrm{on}} - \alpha Y_{\mathrm{off}}$ | $\epsilon$ (%) | $\frac{1}{\sigma_h}\frac{d\sigma}{dp^*} \pm \Delta_{stat} \pm \Delta_{syst}$ |
|---|---|---|---|
| 0.0-0.1 | 289901.7 ± 9256.5 | 18.6 | 4.483 ± 0.143 ± 0.644 |
| 0.1-0.2 | 492207.2 ± 16451.8 | 15.9 | 8.893 ± 0.297 ± 1.182 |
| 0.2-0.3 | 465198.9 ± 10435.8 | 16.5 | 8.106 ± 0.182 ± 1.012 |
| 0.3-0.4 | 461727.6 ± 8139.7 | 20.0 | 6.635 ± 0.117 ± 0.836 |
| 0.4-0.5 | 411074.4 ± 6470.8 | 22.5 | 5.245 ± 0.083 ± 0.699 |
| 0.5-0.6 | 323401.5 ± 5305.1 | 24.8 | 3.749 ± 0.062 ± 0.506 |
| 0.6-0.7 | 255770.0 ± 4409.2 | 26.4 | 2.780 ± 0.048 ± 0.377 |
| 0.7-0.8 | 187946.7 ± 3761.8 | 27.8 | 1.942 ± 0.039 ± 0.290 |
| 0.8-0.9 | 139720.8 ± 3179.7 | 29.3 | 1.370 ± 0.031 ± 0.209 |
| 0.9-1.0 | 106438.9 ± 2754.1 | 30.1 | 1.017 ± 0.026 ± 0.161 |
| 1.0-1.1 | 79213.3 ± 2004.2 | 32.4 | 0.701 ± 0.018 ± 0.125 |
| 1.1-1.2 | 61164.2 ± 1744.7 | 32.8 | 0.535 ± 0.015 ± 0.095 |
| 1.2-1.3 | 46737.0 ± 1528.1 | 33.3 | 0.402 ± 0.013 ± 0.076 |
| 1.3-1.4 | 34688.4 ± 1358.3 | 33.9 | 0.294 ± 0.012 ± 0.059 |
| 1.4-1.5 | 26208.0 ± 1236.0 | 33.7 | 0.223 ± 0.011 ± 0.049 |
| 1.5-1.6 | 18556.8 ± 1115.8 | 35.0 | 0.152 ± 0.009 ± 0.039 |
| 1.6-1.7 | 15916.3 ± 994.5 | 35.5 | 0.129 ± 0.008 ± 0.031 |
| 1.7-1.8 | 12728.9 ± 915.9 | 36.1 | 0.101 ± 0.007 ± 0.026 |
| 1.8-1.9 | 10759.3 ± 805.8 | 37.0 | 0.084 ± 0.006 ± 0.022 |
| 1.9-2.0 | 7842.7 ± 746.8 | 36.7 | 0.061 ± 0.006 ± 0.018 |
| 2.0-2.1 | 7241.3 ± 667.3 | 35.2 | 0.059 ± 0.005 ± 0.017 |
| 2.1-2.2 | 4945.7 ± 586.1 | 32.4 | 0.044 ± 0.005 ± 0.014 |
| 2.2-2.3 | 2956.1 ± 533.1 | 31.2 | 0.027 ± 0.005 ± 0.011 |
| 2.3-2.4 | -345.5 ± 505.8 | 30.7 | -0.003 ± 0.005 ± 0.011 |
| 2.4-2.5 | 163.3 ± 443.3 | 29.7 | 0.002 ± 0.004 ± 0.009 |
| 2.5-2.6 | 488.3 ± 415.3 | 28.4 | 0.005 ± 0.004 ± 0.007 |
| 2.6-2.7 | -242.0 ± 394.3 | 27.2 | -0.003 ± 0.004 ± 0.007 |
| 2.7-2.8 | 189.8 ± 347.3 | 25.5 | 0.002 ± 0.004 ± 0.006 |
| 2.8-2.9 | -206.9 ± 314.9 | 23.7 | -0.003 ± 0.004 ± 0.005 |
| 2.9-3.0 | -59.5 ± 278.8 | 21.6 | -0.001 ± 0.004 ± 0.005 |

TABLE II: Sources of systematic uncertainty in the inclusive $\pi^0$ multiplicity measurement.

| Source | Effect on $\langle n_{\pi^0} \rangle$ (%) |
|---|---|
| Overall normalization | 1.5 |
| $\Delta n = Y_{\rm on} - \left(\frac{\mathcal{L}_{\rm on}}{\mathcal{L}_{\rm off}}\right)\left(\frac{s_{\rm off}}{s_{\rm on}}\right) \cdot Y_{\rm off}$ | 1.5 |
| $R_2$ | 0.4 |
| OFF $E^*_\gamma \cdot \sqrt{\frac{s_{\rm on}}{s_{\rm off}}}$ | 0.3 |
| $E_\gamma$ non-linearity | 0.6 |
| $E_\gamma$ smearing | 2.0 |
| Shower shape | 0.4 |
| Track match | 1.6 |
| Fit procedure | 3.0 |
| Energy dependence of efficiency | 0.3 |
| Total (added in quadrature) | 4.6 |